

Article

Local Heating Networks with Waste Heat Utilization: Low or Medium Temperature Supply?

Hanne Kauko ^{1,*} , Daniel Rohde ¹  and Armin Hafner ²

¹ SINTEF Energy Research, Sem Sælands vei 11, 7034 Trondheim, Norway; daniel.rohde@sintef.no

² NTNU Institute of Energy and Process Technology, Kolbjørn Hejes vei 1B, 7491 Trondheim, Norway; armin.hafner@ntnu.no

* Correspondence: hanne.kauko@sintef.no

Received: 9 January 2020; Accepted: 14 February 2020; Published: 20 February 2020



Abstract: District heating enables an economical use of energy sources that would otherwise be wasted to cover the heating demands of buildings in urban areas. For efficient utilization of local waste heat and renewable heat sources, low distribution temperatures are of crucial importance. This study evaluates a local heating network being planned for a new building area in Trondheim, Norway, with waste heat available from a nearby ice skating rink. Two alternative supply temperature levels have been evaluated with dynamic simulations: low temperature (40 °C), with direct utilization of waste heat and decentralized domestic hot water (DHW) production using heat pumps; and medium temperature (70 °C), applying a centralized heat pump to lift the temperature of the waste heat. The local network will be connected to the primary district heating network to cover the remaining heat demand. The simulation results show that with a medium temperature supply, the peak power demand is up to three times higher than with a low temperature supply. This results from the fact that the centralized heat pump lifts the temperature for the entire network, including space and DHW heating demands. With a low temperature supply, heat pumps are applied only for DHW production, which enables a low and even electricity demand. On the other hand, with a low temperature supply, the district heating demand is high in the wintertime, in particular if the waste heat temperature is low. The choice of a suitable supply temperature level for a local heating network is hence strongly dependent on the temperature of the available waste heat, but also on the costs and emissions related to the production of district heating and electricity in the different seasons.

Keywords: low temperature district heating; waste heat utilization; dynamic modeling

1. Introduction

Heating and cooling in buildings and industry account for approximately 40% of the global final energy demand [1]. While the energy debate continues to have a strong focus on electrification [2], the potential for energy savings in heating and cooling sectors remains largely untapped [1]. At the same time, the increasing degree of urbanization promotes the utilization of collective heating solutions; in Europe, approximately 50% of the buildings' heat demands could be economically met using a network heating system [3,4]. District heating (DH) may thus play a central role in the future fossil-free, smart energy systems [5,6]. A prerequisite for this is a transition from today's high temperature DH systems relying on centralized heat supply plants towards lower distribution temperatures and a higher share of decentralized heat production based on renewable and waste heat sources [4,5,7].

Lowering the distribution temperature provides several advantages. These include for instance reduced distribution heat losses [8,9], as well as a more efficient utilization of low temperature waste heat and renewable heat sources, such as solar thermal and heat pumps [10,11]. Heat pumps are an important link between the thermal and electric energy systems, and increased integration of heat pumps thus supports the use of DH and building heating systems, including thermal storage, as an added dimension for flexibility for the electric grid [12,13]. This will become increasingly important as a growing share of electricity production is moving towards fluctuating renewable sources.

Modern and renovated buildings are well suited for low temperature heat supply [14]; however, heat at high temperature levels is still required at old and non-renovated buildings. The transition to low temperature DH must therefore start from building areas consisting of new or renovated buildings with lower space heating demands. Nevertheless, domestic hot water (DHW) supply still limits the temperature reduction: in Norway, the minimum temperature requirement for DHW preparation is limited to 65 °C by legislation aiming to limit the spread of Legionella [15]. When designing a heat supply system for a new building area, the heat supplier must thus choose between true low temperature (LT) distribution, with DHW production locally at the buildings with, e.g., heat pumps, or medium temperature (MT) distribution at temperature levels able to cover the entire heat demand.

This problem is relevant at Leangen in Trondheim, Norway, where a new residential area will be built. The plan is to utilize condenser waste heat from the dry cooler loop of a nearby indoor ice rink towards a local heating network. Two alternative supply temperature levels are being considered for the local network: LT supply at 40 °C, with DHW production at the customer substations using heat pumps; and MT supply at 70 °C, applying a centralized heat pump to lift the waste heat temperature to the required level. The local network will be connected to the primary high temperature DH network to cover the remaining heating demand. To evaluate the different heat supply alternatives, the local heating network was simulated with the dynamic simulation program Dymola, which is a widely applied tool for detailed physical modeling of DH systems [9,16–18].

The aim of this study is to reveal the advantages and disadvantages of the two supply temperature alternatives in terms of heat and electricity use, considering both heat import from the primary DH network as well as electricity required for circulation pumps and compressors of the heat pumps. The ultimate goal is to provide decision support to energy companies, real estate developers and municipalities for creating holistic energy supply solutions with low total and peak energy demands for new building areas.

2. Methodology

2.1. The Building Area

Leangen is a new building area to be built in Trondheim on the land of a previous trotting rink. Figure 1 shows an architectural illustration of the area, together with a sketch for the planned local heating network. The construction work will be carried out in three stages; the first stage is expected to start in 2022, and the area is expected to be fully built within 15–20 years. The building mass will consist mainly of apartment blocks; however, a number of other building types will be present as well, as shown in Table 1. Apart from apartment blocks and a nursing home, the final share of the heated area of other building types is not fully decided yet, and the values given in Table 1 for these remaining building types are thus estimates. The total heated area will be 183,000 m², and the total size of the building area is 120 daa (1.2 ha). The area will be very tightly built, in line with the directions for urban area planning in Trondheim. The total length of the piping network was estimated to 1.6 km.

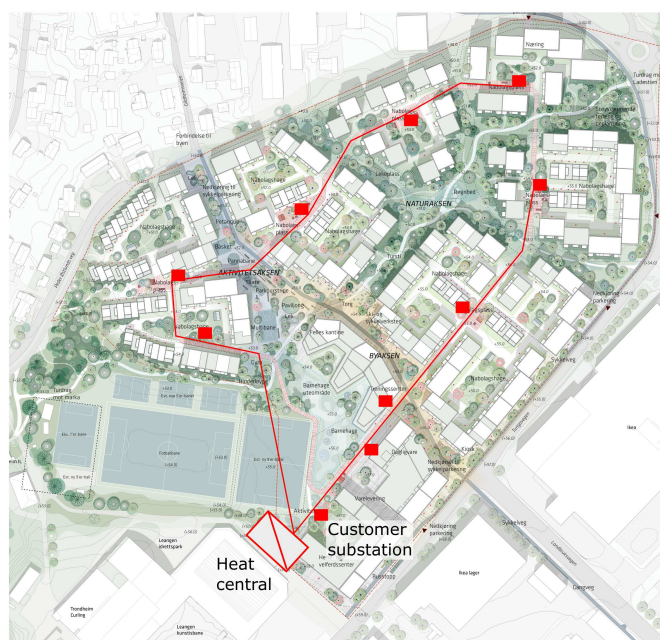


Figure 1. Architectural illustration of the planned building area at Leangen (scale 1:1000, obtained with permission from [19]), together with a sketch of the planned local heating network.

Table 1. The building mass to be built at Leangen, together with the calculated annual specific space and domestic hot water (DHW) heating demand.

Building Type	Heated Area [m ²]	Space Heating Demand [kWh/m ² /year]	DHW Heating Demand [kWh/m ² /year]
Apartment	139,300	32	30
Nursing home	12,000	94	46
Office	12,000	27	10
Nursery	2000	102	39
Commercial	9000	71	27
Sports	8700	27	5
Total	183,000	—	—

Heat demand data for the building area were obtained using a load profile generator developed by Lindberg et al. [20]. The load profile generator builds up on a large database of measurement data on the heating demand for buildings from different categories from all over Norway. The data are converted into a correlation for the heating demand as a function of ambient temperature using data regression models. The load profile generator calculates the hourly energy demands for heating of space and DHW, with the heated area for each building type and data for outdoor temperature as an input. For outdoor temperature, a representative year for design obtained from the building simulation program SIMIEN was used [21].

The buildings at Leangen will be built according to the latest building standards. However, since a sufficient amount of data for new energy efficient buildings for reliable load prediction are not yet available for all building types, the heating demand for commercial buildings, nurseries and nursing homes was based on data for regular buildings. The resulting specific energy demands were still close to the values given by the latest building regulations in Norway [22]. Moreover, the heat demand profile for sports buildings was generated using the correlation for modern school buildings due to lack of data on heating

demand for sports buildings, which generally varies greatly. The resulting total annual heat demand for the area was 12.1 GWh, yielding a linear heat demand density of 7.55 MWh/year per meter trench.

2.2. The Waste Heat Source

At Leangen, an indoor ice skating rink is present, with approximately 3 GWh waste heat available annually over the winter months when the facility is running. The facility is closed over three months in the summer, from the end of April until the start of August. Hourly data for the amount of heat rejected through the dry coolers were obtained from the operator of the facility, the Municipality of Trondheim, from start of January until the start of December 2018. In the simulations, the entire year of 2018 was nevertheless evaluated, assuming that there was no waste heat available in December. The temperature of the waste heat at the dry coolers is approximately 30 °C. The waste heat source being large ammonium cooling machines, an option with waste heat temperature of 35 °C was additionally evaluated, implying a corresponding increase in the condensing temperature for the cooling machines.

2.3. Modeling Approach

The local heating network was modelled using the dynamic simulation software Dymola (DYnamic MOdeling LAboratory) [23] and the object-oriented modeling language Modelica. For a more detailed description of the chosen modeling approach, see [18]. The network model was built using an in-house component library created in previous projects [18,24]. Important component models applied in the present study are, e.g., the heat exchanger model based on the effectiveness–NTU method [24]; twin-pipe model based on correlations from [25], described in [18]; as well as the heat pump model, described in Section 2.3.2.

2.3.1. The Network Model

Figure 2 shows the local heating network as modelled in Dymola. The network consists of the building stock, i.e., customer substations for different types of buildings; a heat centre delivering the required amount of heat; and a piping network distributing the heat, divided in two branches. The building area was modelled as 10 buildings: 5 apartment blocks, a nursing home, a kindergarten, an office building, a retail store, and a sports building. Each building in the network has an identical substation, but different input data, as well as different dimensions for heat exchangers etc. The layout of the customer substation, as well as the layout of the heat centre is however different for the two cases with different supply temperature levels, as will be explained in Section 2.4.

The heat centre ensures that heated water at the required temperature and pressure level is supplied to the system at each moment. The required pressure lift is determined by the buildings furthest away from the central, with the objective of maintaining the pressure drop at a minimum of 70 kPa for these customers, as explained in [18]. The maximum pressure lift from the heat centre was limited to 1 MPa.

The pipe diameters were selected assuming a maximum pressure drop of 150 Pa/m and using a relationship between maximum mass flow rate \dot{m}_{max} and inner diameter D_i derived in [26]:

$$D_i = 0.0379 \cdot \dot{m}_{max}^{0.37} \quad (1)$$

The equation thus gives the inner pipe diameter at a pressure drop of 150 Pa/m, based on a given maximum mass flow rate in each pipe. The pipe diameters applied in the model were obtained by rounding the resulting value up to the nearest real diameter available from DH pipe suppliers [27].

The maximum mass flow rate for each pipe was selected using results from a test simulation run, carried out for each case. The resulting mass flow rates for the LT case were two to three times higher than

in the MT case. The dimensioning mass flow rates and the resulting inner pipe diameters applied in the model are shown in Table 2, together with the pipe lengths.

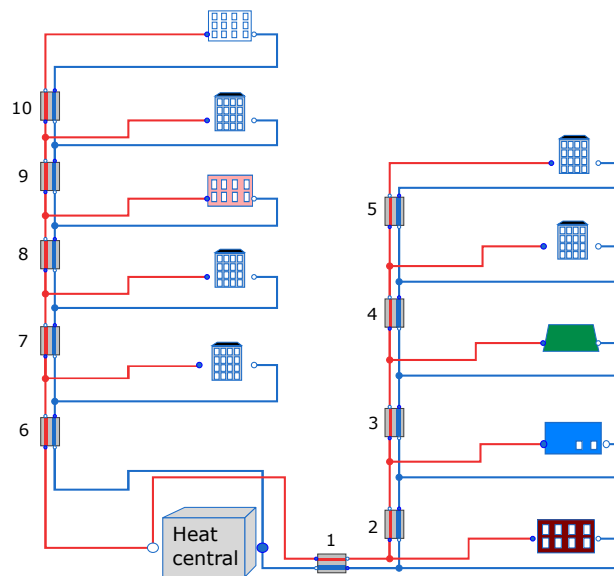


Figure 2. A schematic of the model in Dymola, consisting of a heat centre and two network branches supplying heat to 10 buildings: 5 apartment blocks, a nursing home, a kindergarten, an office building, a retail store and a sports building.

Table 2. The pipe lengths, selected dimensioning mass flow rates and resulting inner pipe diameters for the low temperature (LT) and medium temperature (MT) case. The pipe numbering is as shown in Figure 2.

Pipe	Length [m]	LT		MT	
		\dot{m}_{max} [kg/s]	D_i [mm]	\dot{m}_{max} [kg/s]	D_i [mm]
1	50	40	200	15	125
2	100	30	150	10	100
3	100	20	125	8	100
4	150	20	125	8	100
5	200	10	100	4	65
6	300	40	150	15	125
7	100	30	150	10	100
8	100	16	125	5	80
9	300	15	125	5	80
10	200	4	65	2	50

2.3.2. Heat Pump Model

Heat pump will be a key technology in future integrated energy systems by serving as a link between the thermal and electric energy systems. The heat pump model applied in this study is based on the theoretical Lorentz cycle, explained in detail in [24]. The primary side, i.e., the cycle of the working fluid is not modelled, but the evaporator and condenser heat flow rate as well as the compressor power are calculated using the Lorentz COP (COP_L), which depends on the inlet and outlet temperatures on the secondary sides. The heat pump's COP (COP_{HP}) is calculated by multiplying COP_L with a constant Lorentz efficiency (η_L).

Two types of heat pumps are considered in the study: transcritical CO₂ heat pumps for DHW production in the LT case (see Section 2.4.1), and an NH₃ heat pump to upgrade the temperature of the

waste heat in the MT case (Section 2.4.2). Heat pumps using the environmentally benign working fluid CO₂ on a transcritical cycle are particularly well suited for DHW production owing to the temperature glide in the gas cooler, matching well with the heating curve of water [28]. This together with the good heat transfer characteristics of CO₂ enable a high heat pump efficiency. For large-scale heat production and waste heat recovery, NH₃ heat pump provides an efficient and environmentally friendly alternative [29,30]. NH₃ heat pumps are successfully applied for DH production in, e.g., Denmark and Norway [31].

To make sure that the chosen Lorentz efficiency yielded correct COP_{HP}, and thus realistic heat flow rates and compressor work for each case, steady-state CO₂ and NH₃ heat pump models were additionally developed in Excel. These steady-state models considered all the relevant stages of the heat pumping cycle, and were applied to cross-check that the outputs of the heat pump model in Dymola were within the correct range with respect to the intended evaporation and gas cooler/condenser temperatures and pressures. The applied values for η_L were 0.16 for the NH₃ heat pump and 0.19 for the CO₂ heat pumps.

2.4. Case Study Description

Figure 3 shows schematic diagrams of the heat centre coupled to one substation, with a twin pipe in between, for the LT and MT case. These two cases were analyzed with the two alternative waste heat temperature levels, resulting in four simulated cases, described in Table 3. As the supply temperature is in both LT and MT cases at the minimum level to be able to cover the temperature requirements for space and DHW heating, constant supply temperatures were applied throughout the year. The chosen layouts for the customer substation and heat centre represent possible system solutions that are being considered for Leangen.

Table 3. The four simulated cases, corresponding to the two different supply temperature alternatives (T_{supply}) and two waste heat temperatures (T_{wh}).

	$T_{supply} = 40\text{ }^{\circ}\text{C}$	$T_{supply} = 70\text{ }^{\circ}\text{C}$
$T_{wh} = 30\text{ }^{\circ}\text{C}$	LT 30	MT 30
$T_{wh} = 35\text{ }^{\circ}\text{C}$	LT 35	MT 35

2.4.1. Low Temperature Supply: Decentralized DHW Production

In the customer substation for the LT supply case, the space heating heat exchanger supplies a floor heating loop with a temperature set-point of 35 °C, and is coupled in series with the evaporator of a DHW heat pump. In the summertime, when space heating demand is small, a by-pass pump is applied to maintain a minimum evaporator outlet temperature of 20 °C and thus a sufficient mass flow through the heat pump evaporator (see Figure 3).

The DHW heat pump is coupled to hot water storage tanks, dimensioned to have a sufficient capacity such that the heat pump can be operated at a constant and low output. This will enable lower installed heat pump capacity, and thus reduced investment costs and a lower peak load on the power grid. Nevertheless, to allow fair comparison with the MT case, an option with instantaneous DHW heating with the heat pump was also evaluated (see Section 4). The necessary daily storage volume for each building was calculated from an average total daily DHW demand using the previously obtained heat demand data. The hot water tank itself was not modelled; instead, a constant mass flow rate enabling the required accumulation was applied on the condenser side. The DHW supply set-point temperature was in this case set to 85 °C due to the accumulation of the water, to prevent the growth of Legionella as well as to account for heat losses from the tank. The temperature of the return water was set to 10 °C.

In the heat centre, the network receives heat first from the waste heat source, and thereafter from the primary DH network to obtain the desired supply temperature level. The mass flow rate and temperature

levels of the waste heat and DH supply on the primary side were not of interest for the present case, and the heat inputs were thus modelled as pipes with heat exchange. For the two different waste heat temperature levels considered in the study, 30 and 35 °C, the temperature of the network water at the heat exchanger outlet, $T_{WHhx,out}$, was set to 28 and 33 °C, respectively. The heat input from the waste heat source is thus calculated from

$$\dot{Q}_{WHin,40} = \min (\dot{Q}_{WHdata}, \dot{m} \cdot C_p (T_{WHhx,out} - T_{return})) , \tag{2}$$

where \dot{Q}_{WHdata} is the data for available waste heat, \dot{m} is the mass flow rate at the heat centre, C_p is the specific heat capacity of water, and T_{return} is the return temperature from the network. This equation ensures that the waste heat source heats the water only up to the temperature set for $T_{WHhx,out}$. Furthermore, only positive values are allowed; that is, if $T_{WHhx,out} < T_{return}$, the heat input from the waste heat source is set to zero.

The heat flow rate for DH delivered to the local network, \dot{Q}_{DH} , is calculated from

$$\dot{Q}_{DH} = \dot{m} \cdot C_p (T_{supply} - T_{DHhx,in}) , \tag{3}$$

where T_{supply} is the supply temperature in the network (40 °C), and $T_{DHhx,in}$ is the temperature of the water at the inlet of the DH heat exchanger.

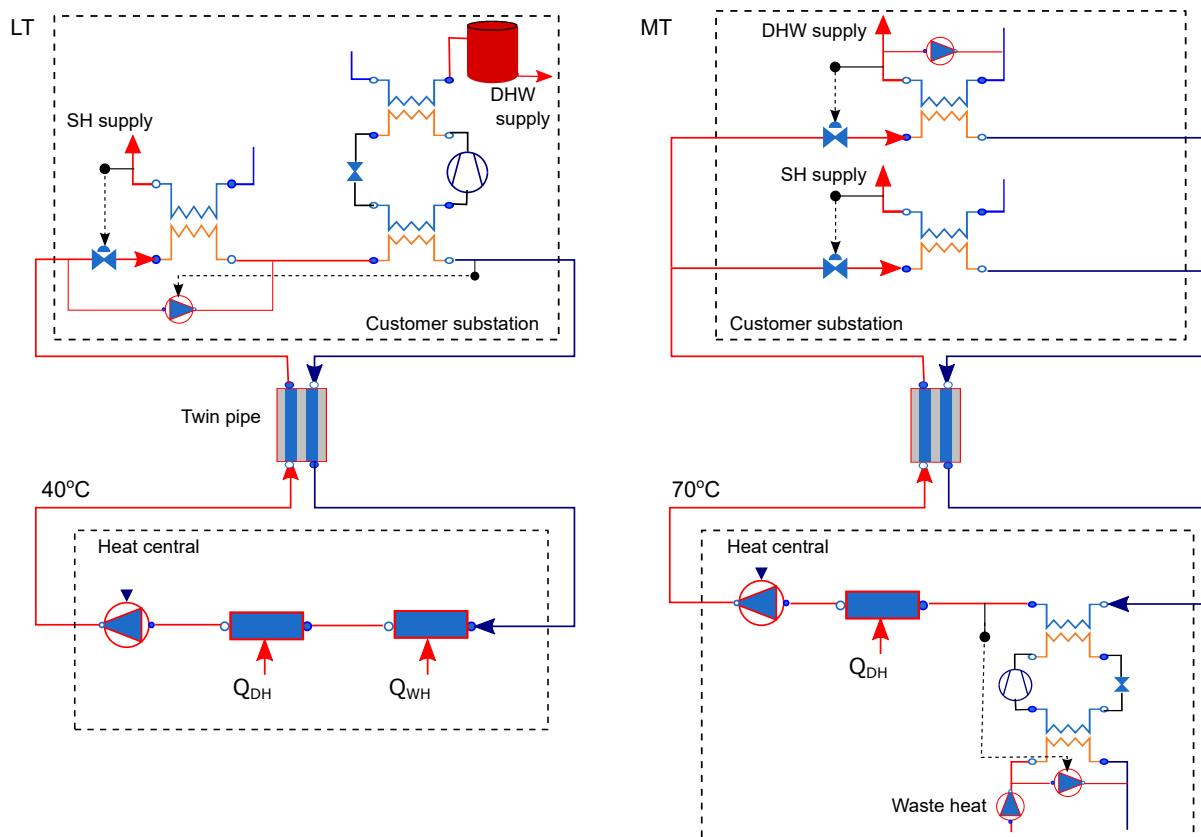


Figure 3. A schematic of the heat centre coupled to one substation with a twin pipe in between for the LT and MT supply case.

2.4.2. Medium Temperature Supply: Centralized Heat Pump

In the MT case, a conventional DH substation with heat exchangers for space and DHW heating coupled in parallel is applied. The space heating heat exchanger supplies a floor heating loop with a temperature set-point of 35 °C, similarly to the LT case. The DHW demand is in this case supplied with an instantaneous heat exchanger, and the temperature set-point for DHW was set to 65 °C.

Most large buildings have a circulation system for DHW to ensure short waiting time for warm water at the tap, as well as to reduce the risk for bacterial growth due to warm water standing still at the pipes. A circulation pump was therefore included in the DHW heat exchanger (see Figure 3), with the flow rate estimated from the basis of measurements on existing buildings [32]. This circulation increased the temperature of the incoming city water on the secondary side and thus ensured realistic return temperatures from the DHW heat exchangers to the network.

The dimensions of the space and DHW heat exchangers, and in the LT case the DHW heat pump evaporator, were chosen based on the maximum heat demands and considering the desired return temperatures at the heat centre. The targeted return temperature was 40 °C for the MT case, and 25 °C for the LT case.

In the heat centre, the waste heat source supplies heat to the evaporator of an NH₃ heat pump, upgrading the temperature of the waste heat. The temperature of the waste heat at the evaporator inlet was set to the temperature of the waste heat source (30 or 35 °C), and it was assumed that the evaporator would cool the water down by 10 K. The evaporation temperature was assumed to be 15 and 20 °C for the two different waste heat temperature levels, corresponding to a temperature pinch of 5 K at the evaporator outlet. The heat input to the evaporator was regulated through the mass flow, calculated from the data for available waste heat and a temperature difference of 10 K. The heat pump was additionally equipped with a by-pass pump ensuring that the condenser outlet temperature does not exceed 70 °C, shown in Figure 3.

Similarly to the 40 °C case, heat is supplied from the primary DH network if needed, to obtain a supply temperature of 70 °C. The required heat flow rate for DH delivered to the local network is calculated according to Equation (3), now with $T_{supply} = 70$ °C.

3. Results

3.1. Total Energy Demands

Table 4 shows the total annual heat demands, the heat supply as well as the electricity use for compressors and pumps for the four simulated cases. The total DHW demand shown for the LT case is the heat supplied to the heat pump evaporator. The heat losses are small, less than 2% of the total heat demand for both cases owing to the high heat demand density; nevertheless, the losses for LT case are 41% lower than for the MT case.

For the LT case, higher waste heat temperature results in a clear increase in the amount of waste heat supply and correspondingly a decrease in the DH supply to the local network. The electricity use for the DHW heat pump compressors and circulation pumps is not affected by the waste heat temperature. For the MT case, both the delivered waste heat and delivered DH increase somewhat as a result of increased waste heat temperature; however, the electricity use for the waste heat pump compressor decreases drastically due to increased COP. The sum of energy input to the system—waste heat, DH and electricity—is for both cases the same irrespective of waste heat temperature. This, in the MT case, increased waste heat temperature results in an increased share of the total energy demand being covered by heat. Note that the delivered waste heat shown for MT case in Table 4 is the heat input to the heat pump evaporator, not the heat delivered to the local network.

The total amount of waste heat available for 2018 was 3078 MWh based on the data. The LT case is thus able to utilize 25%/79% of this heat with the lower/upper waste heat temperature level, respectively, and the MT case is able to utilize 90%/92% of the heat.

Table 4. The total annual energy in- and outputs for the LT and MT cases, for the two different waste heat temperatures: total heat demand for space and DHW heating as well as heat losses; heat supply from waste heat and DH; and electricity use for compressors and pumps.

		LT		MT		
Heat demand [MWh]	Heat loss	99.5		173.6		
	Space heating	6948		6948		
	DHW	3965		5201		
	Total	11,013		12,323		
		T_{wh} [°C]	30	35	30	35
Heat supply [MWh]	Waste heat	780	2428	2780	2834	
	District heating	10,234	8585	8086	8341	
	Total	11,013	11,013	10,866	11,175	
Electricity use [MWh]	Compressor	1243	1243	1456	1148	
	Pump	86	86	34	34	
	Total	1328	1328	1 491	1182	
Total energy supply [MWh]		12,342	12,342	12,357	12,357	

Figure 4 shows the heat supply and electricity use as bar graphs for the four different cases, illustrating how these energy inputs are affected by the waste heat temperature. With lower supply temperature, the waste heat temperature level is critical for the ability to directly utilize the waste heat source. Thus for the LT supply case, the waste heat temperature level is determinant for the amount of waste heat and DH supplied to the network, as can be seen from Figure 4. When the waste heat is upgraded with a heat pump, as is done in the MT case, the waste heat temperature affects first of all the electricity use of the heat pump, while the heat supply is little affected. Note, however, that the electricity use is an order of magnitude lower than the heat supply.

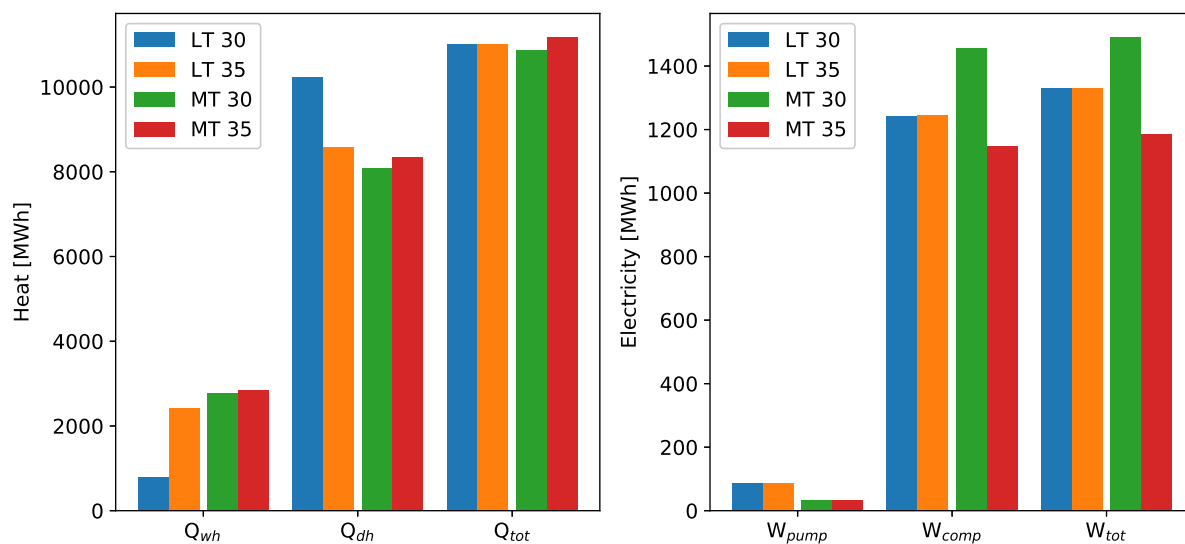


Figure 4. The heat supplied through waste heat and DH (left) and electric energy for pumps and compressors (right) for the LT and MT cases with waste heat temperatures of 30 and 35 °C.

The pump work for circulation pumps is in both cases independent of the waste heat temperature, and small with respect to the compressor work. The pump work in the LT case is approximately twice as high as in the MT case. The compressor work and hence the total electricity use is higher for the MT case than for the LT case with a lower waste heat temperature, and vice versa for the higher waste heat temperature. The lower electricity use for the MT case results from the fact that there was no waste heat available during the summer months and in December as explained in Section 2.1, hence no compressor use for the MT case during these periods. This is can be clearly seen from Figures 5 and 6.

3.2. Hourly Heat and Electricity Demands

Figure 5 shows how the total energy use for the local heating network is allocated to the different energy sources throughout the year: electricity (divided between electricity use for compressors and pumps), DH and waste heat. For the LT case, DH covers a major part of the total energy use, in particular at the lower waste heat temperature level. Increased waste heat temperature reduces the share of DH, in particular in the winter months. The electricity use is rather constant throughout the year owing to the constant power consumption of the DHW heat pumps; however, the share of electricity use is higher during the summertime, when the space heating demand is low.

For the MT case, waste heat covers a larger share, up to 60%, of the total energy use in the winter time when waste heat is available. On the other hand, the compressor electricity use is also high in the wintertime, with peak demands reaching up to 40% of the total energy use with the lower waste heat temperature level, and ca. 35% with the higher waste heat temperature level. During the summer when no waste heat is available, DH covers the entire energy demand and the electricity use is minimal. This profile fits well to DH systems that have excess production in the summertime, such as systems with waste incineration or solar heat as the base load. The electricity use for pumps is negligible for both cases, in particular for the MT case.

Figure 6 shows the duration curves for heat and electricity supply for all the four cases. The duration curve for heat supply is similar for both LT and MT cases, and not affected by the waste heat temperature, as the same heat demand data were applied in each case. The LT case has slightly lower peak heating demand than the MT case (4348 kW as opposed to 4705 kW) owing to the use of accumulation tanks for DHW production. For the same reason, the duration curve for the LT case flattens out at ca. 7000 h.

The difference in electricity use is however significant. The MT case has clearly higher peak power demand, with 1163 kW for the lower, and 992 kW for the higher waste heat temperature level. For the LT case, the peak power demand is 367 kW. The electricity use is in the LT case not affected by the waste heat temperature level, thus the two curves in Figure 6 (LT 30 and LT 35) lie on top of each other. The reason for the higher peak power demand, and generally higher electricity demand most of the year for the MT case, is that the waste heat heat pump works to increase the temperature level for the entire heat demand in the network. This includes both space and DHW demands, even if the space heating does not require heat at such high temperature levels.

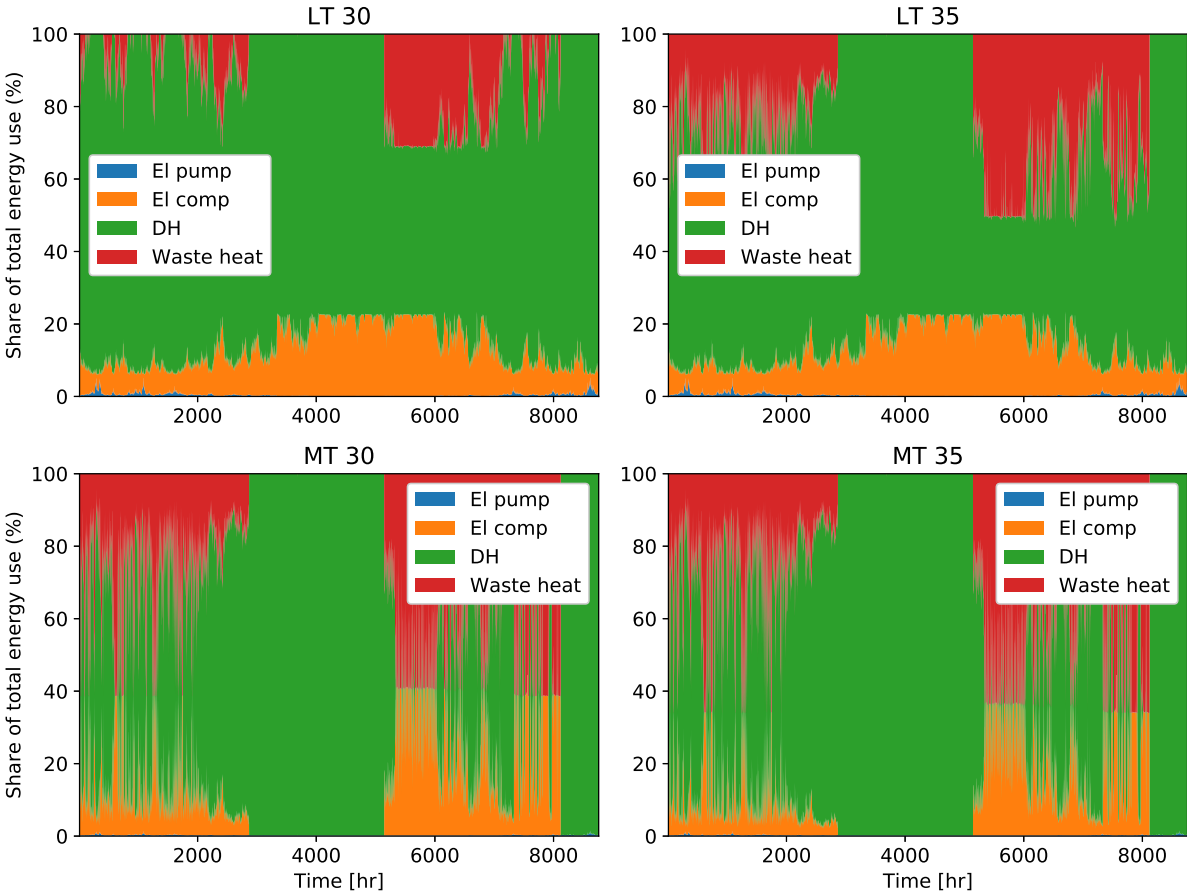


Figure 5. The share of the total energy use of the local heating network covered by the different energy sources for the four simulated cases.

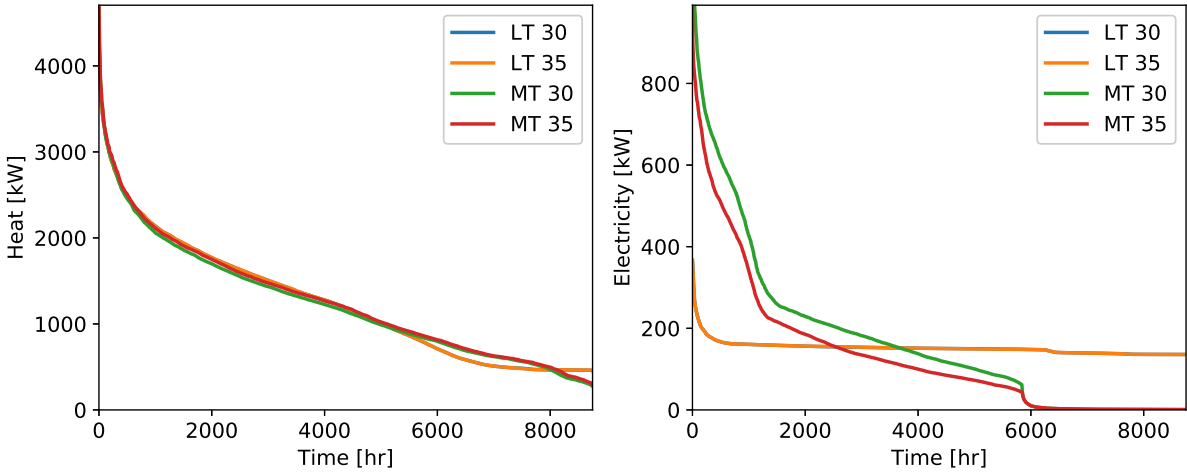


Figure 6. The duration curves for heat (left) and electricity (right) for the four simulated cases. The duration curve for heat includes the supply by both waste heat and DH; and the curve for electricity includes the use to both compressors and pumps.

4. Discussion

The simulation results show a clear difference in the heat and electricity use for the two different supply temperature alternatives for the studied local heating network. In the LT supply alternative, where electricity is utilized primarily by heat pumps producing DHW, most of the total energy use in the network is supplied by heat (waste heat or DH). The share between these two heat sources is strongly dependent on the waste heat temperature level. Nevertheless, the largest share of the total energy use is covered by DH.

In the MT supply alternative, where a heat pump is applied to upgrade the waste heat temperature to supply heat at a higher temperature for the entire network, waste heat covers a larger share of the entire energy demand, in particular in the winter time. The electricity use in the wintertime is, however, high, with peak power demands up to 3.2 times higher than in the LT supply case. Higher waste heat temperature reduces the electricity use, resulting from a higher heat pump COP.

The choice of suitable supply temperature level for a local heating network is hence strongly dependent on the temperature of the available waste heat, but also on the prices for DH and electricity, as well as the emissions related to the production of these in the different seasons. The high peak power demands in the MT case occur in the wintertime, when the demand in the electric grid is generally high. On the other hand, in the LT case the peak DH demand from the primary network is high, in particular if the temperature of the waste heat is low. High peak DH demand for a new building area will increase the use of peak heating boilers in the DH network, which will increase the costs and emissions related to DH production.

An increase in the waste heat temperature is, in the present study, related to increased condensing temperature of the chiller system of a nearby ice skating rink. Assuming an evaporation temperature of $-5\text{ }^{\circ}\text{C}$, a 5 K increase in the condensing temperature would imply a ca. 12% increase in the compressor power demand for the chiller system. Considering the high peak power demand for the MT case, and the improved possibilities for waste heat utilization for the LT case with higher waste heat temperature, a 12% increase in the compressor work for the skating rink chiller system might be a well justified solution for the favour of a LT supply system.

The electricity use for both LT and MT case is obviously strongly dependent on the COP_{HP} of the DHW and waste heat heat pumps, respectively, which is determined by the chosen Lorentz efficiency in the heat pump model (see Section 2.3.2). The average COP_{HP} was 4.17 for the LT case (average COP for all DHW heat pumps), and 3.12 and 3.89 for the waste heat heat pump in the MT case for the lower and higher waste heat temperature, respectively. The design point COP_{HP} based on the steady-state models was 4.61 for the LT case, and 3.87/4.25 for the MT case for the low/high waste heat temperature levels. Nevertheless, although the Lorentz efficiency is an important parameter regarding the electricity use, the main reason for the high peak power demand for the MT case is that the waste heat heat pump works to increase the temperature level in the entire network, as mentioned in Section 3.2. In the LT case, the heat pumps work only to cover the DHW demands, which covers less than half of the total heat demand (see Table 4). Indeed, better match with the supply temperature for space heating in the LT case leads to lower exergy loss as was pointed out by Li and Svendsen [33], yielding lower electricity demand.

For the LT case, the use of DHW accumulation tanks may have affected the peak heating and power demands, and the option of instantaneous DHW production was therefore investigated in addition. Having no storage tank increased the peak power demand in the LT case by 14%, to 416 kW, which is still clearly lower than the peak power demand in the MT case. The peak heating supply was increased by 4%, to 4526 kW.

In a LT network, low return temperature at the heat centre is extremely important to enable good utilization of the waste heat source as well as low mass flow rates. Obtaining low return temperatures is dependent on a proper design of the space heating loop, which is thus crucial in low temperature DH,

as was pointed out by Schmidt et al. [7]. In the present study, the space heating heat exchanger areas used in the simulations for the LT case were nine times as high as those applied for the MT case. In addition to larger heat exchangers, larger pipes are needed in LT distribution (see Table 2).

The investment costs for the LT alternative are hence expected to be higher than for the MT alternative, not only due to larger heat exchangers and pipes, but also due to a number of DHW heat pumps required at the customer substations. Based on a dialogue with a potential supplier, the price for a CO₂ DHW heat pump unit is EUR 28,000 with a heating capacity of 50 kW, and EUR 39,000 with a capacity of 100 kW [34]. According the current building plan for Leangen, ten 50 kW units and two 100 kW units will be required, yielding a total investment cost of EUR 106,010, excluding the costs for hot water storage tanks. For the MT case, an NH₃ heat pump for upgrading the waste heat with a heating capacity of minimum 2 MW would be needed. The price of such a unit was estimated to be EUR 295,000 [35], which is nearly three times the investment costs for the heat pumps in the LT case. A more detailed techno-economic analysis of the suggested LT alternative will be carried out in a separate spin-off project.

The potential of low temperature DH for similar, confined and new building areas as investigated in this study has been identified widely and such systems have been implemented in several locations in Europe (see, e.g., [7]). Lowering the distribution in the existing distribution network is however challenging due to, e.g., limited capacity in pipes and heat exchangers [36]. Low temperature DH may also be less profitable in areas with low heat demand density [37].

5. Conclusions

In this study, a comparison between low (40 °C) and medium temperature (70 °C) supply for a local heating network has been successfully analysed using dynamic simulations. The study is related to the development of a heat supply solution for a new building area in Trondheim, Norway. The planned heat sources are waste heat from a nearby ice skating rink, and the primary DH network. For the waste heat source, two different temperature levels, 30 and 35 °C, were analysed. In the LT case, the customer substations were equipped with CO₂ heat pumps for DHW production, while in the MT case, a centralized NH₃ heat pump was applied to upgrade the temperature of the waste heat.

The study shows that the choice of a suitable supply temperature level for a local heating network is strongly dependent on the temperature of the available waste heat, but also on the prices and emissions related to the production of DH and electricity in the different seasons. With LT supply, demand for DH from the primary network is high in the wintertime, in particular if the waste heat temperature is low. With MT supply on the other hand, high electricity demands occur in the wintertime, when the demand in the electric grid is generally high. The peak power demand for the MT case was 2.7 to 3.2 times higher than for the LT case, with lower values being related to higher waste heat temperatures. In the MT case, the waste heat heat pump works to increase the temperature level in the entire network, including both space and DHW demands, even if space heating does not require heat at such high temperatures. In the LT case, the heat pumps work only to cover the DHW demands, which results in a low and even electricity demand. The study thus demonstrates that decentralized DHW production with heat pumps contributes to a low load on the electric grid, in particular when combined with hot water storage. With sufficient storage capacity, the heat pump may also be shut down during peak power periods, thereby supporting a flexible interaction between thermal and electric grids.

Another aspect that favors LT supply is significantly lower heat losses (by 41%), although heat losses in a small network as considered in this study are nevertheless small (below 2%). Moreover, low temperature distribution enables connecting several waste heat sources, such as condenser heat from food retail stores or data centres, to the local network later on, thus increasing the reliability of heat supply and reducing the dependency on the primary DH network.

Author Contributions: Conceptualization, H.K. and A.H.; methodology, H.K. and D.R.; software, D.R. and H.K.; formal analysis, H.K.; investigation, H.K.; resources, H.K. and D.R.; data curation, H.K.; writing—original draft preparation, H.K.; writing—review and editing, H.K. and D.R.; visualization, H.K. and D.R.; supervision, A.H.; project administration, H.K.; funding acquisition, H.K. All authors have read and agreed to the published version of the manuscript.

Funding: This research was funded by The Research Council of Norway under grant number 280994.

Conflicts of Interest: The authors declare no conflict of interest. The funders had no role in the design of the study; in the collection, analyses, or interpretation of data; in the writing of the manuscript, or in the decision to publish the results.

Abbreviations

The following abbreviations are used in this manuscript:

DH	District heating
DHW	Domestic hot water
LT	Low temperature
MT	Medium temperature
WH	Waste heat

References

1. International Energy Agency. *Energy Technology Perspectives 2017—Executive Summary*; International Energy Agency (IEA) Publications: Paris, France, 2017; p. 371.
2. Capuano, L. *International Energy Outlook 2018 (IEO2018)*; US Energy Information Administration (EIA): Washington, DC, USA, 2018; Volume 2018, p. 21.
3. Connolly, D.; Mathiesen, B.V.; Østergaard, P.A.; Möller, B.; Nielsen, S.; Lund, H.; Persson, U.; Nilsson, D.; Werner, S.; Trier, D. *Heat Roadmap Europe 2050: First Pre-Study for the EU27*; Euroheat & Power: Hartford, CT, USA, 2012.
4. Connolly, D.; Lund, H.; Mathiesen, B.V.; Werner, S.; Möller, B.; Persson, U.; Boermans, T.; Trier, D.; Østergaard, P.A.; Nielsen, S. Heat Roadmap Europe: Combining district heating with heat savings to decarbonise the EU energy system. *Energy Policy* **2014**, *65*, 475–489. [[CrossRef](#)]
5. Lund, H.; Werner, S.; Wiltshire, R.; Svendsen, S.; Thorsen, J.E.; Hvelplund, F.; Mathiesen, B.V. 4th Generation District Heating (4GDH): Integrating smart thermal grids into future sustainable energy systems. *Energy* **2014**, *68*, 1–11. [[CrossRef](#)]
6. Connolly, D.; Lund, H.; Mathiesen, B. Smart Energy Europe: The technical and economic impact of one potential 100% renewable energy scenario for the European Union. *Renew. Sustain. Energy Rev.* **2016**, *60*, 1634–1653. [[CrossRef](#)]
7. Schmidt, D.; Kallert, A.; Blesl, M.; Svendsen, S.; Li, H.; Nord, N.; Sipilä, K. Low temperature district heating for future energy systems. *Energy Procedia* **2017**, *116*, 26–38. [[CrossRef](#)]
8. Dalla Rosa, A.; Christensen, J.E. Low-energy district heating in energy-efficient building areas. *Energy* **2011**, *36*, 6890–6899. [[CrossRef](#)]
9. Köfinger, M.; Basciotti, D.; Schmidt, R.; Meissner, E.; Doczekal, C.; Giovannini, A. Low temperature district heating in Austria: Energetic, ecologic and economic comparison of four case studies. *Energy* **2016**, *110*, 95–104. [[CrossRef](#)]
10. Brange, L.; Englund, J.; Lauenburg, P. Prosumers in district heating networks—A Swedish case study. *Appl. Energy* **2016**, *164*, 492–500. [[CrossRef](#)]
11. Ommen, T.; Markussen, W.B.; Elmegaard, B. Lowering district heating temperatures—Impact to system performance in current and future Danish energy scenarios. *Energy* **2016**, *94*, 273–291. [[CrossRef](#)]
12. Münster, M.; Morthorst, P.E.; Larsen, H.V.; Bregnbæk, L.; Werling, J.; Lindboe, H.H.; Ravn, H. The role of district heating in the future Danish energy system. *Energy* **2012**, *48*, 47–55. [[CrossRef](#)]

13. Masy, G.; Georges, E.; Verhelst, C.; Lemort, V.; André, P. Smart grid energy flexible buildings through the use of heat pumps and building thermal mass as energy storage in the Belgian context. *Sci. Technol. Built Environ.* **2015**, *21*, 800–811. [[CrossRef](#)]
14. Brand, M.; Svendsen, S. Renewable-based low temperature district heating for existing buildings in various stages of refurbishment. *Energy* **2013**, *62*, 311–319. [[CrossRef](#)]
15. Direktoratet for Byggkvalitet. *Byggteknisk Forskrift (TEK 10): Veiledning om Tekniske krav til Byggverk*; Technical Report; Direktoratet for Byggkvalitet: Oslo, Norway, 2011.
16. Giraud, L.; Bavière, R.; Vallée, M.; Paulus, C. Presentation, Validation and Application of the District Heating Modelica Library. In Proceedings of the 11th International Modelica Conference, Versailles, France, 21–23 September 2015; Linköping University Electronic Press: Linköping, Sweden, 2015.
17. Schweiger, G.; Larsson, P.O.; Magnusson, F.; Lauenburg, P.; Velut, S. District heating and cooling systems—Framework for Modelica-based simulation and dynamic optimization. *Energy* **2017**, *137*, 566–578. [[CrossRef](#)]
18. Kauko, H.; Kvalsvik, K.H.; Rohde, D.; Nord, N.; Utne, Å. Dynamic modeling of local district heating grids with prosumers: A case study for Norway. *Energy* **2018**, *151*, 261–271. [[CrossRef](#)]
19. Koteng Jenssen AS. Leangen Bolig. 2019. Available online: <https://www.koteng.no/leangenbolig/> (accessed on 16 December 2019).
20. Lindberg, K.; Bakker, S.; Sartori, I. Modelling electric and heat load profiles of non-residential buildings for use in long-term aggregate load forecasts. *Util. Policy* **2019**, *58*, 63–88. [[CrossRef](#)]
21. ProgramByggerne ANS. SIMIEN Wiki. 2020. Available online: <https://www.programbyggerne.no/SIMIEN/> (accessed on 23 January 2020).
22. Direktoratet for Byggkvalitet. Dette er Energikravene i Byggteknisk Forskrift. 2018. Available online: <https://dibk.no/verktoy-og-veivisere/energi/dette-er-energikravene-i-byggteknisk-forskrift/> (accessed on 19 November 2019).
23. Scansot. Dymola. 2020. Available online: <https://scanscot.com/products/systems-engineering/dymola/> (accessed on 9 January 2020).
24. Rohde, D.; Andresen, T.; Nord, N. Analysis of an integrated heating and cooling system for a building complex with focus on long-term thermal storage. *Appl. Therm. Eng.* **2018**, *145*, 791–803. [[CrossRef](#)]
25. Wallentén, P. *Steady-State Heat Loss from Insulated Pipes*; Report TVBH-3017; Department of Building Physics, Lund Institute of Technology: Lund, Sweden, 1991.
26. Kauko, H.; Kvalsvik, K.; Rohde, D.; Hafner, A.; Nord, N. Dynamic modelling of local low temperature heating grids: A case study for Norway. *Energy* **2017**, *139*, 289–297. [[CrossRef](#)]
27. Logstor. 2017. Available online: <https://www.logstor.com> (accessed on 31 May 2017).
28. Nekså, P.; Rekstad, H.; Zakeri, G.R.; Schiefloe, P.A. CO₂-heat pump water heater: Characteristics, system design and experimental results. *Int. J. Refrig.* **1998**, *21*, 172–179. [[CrossRef](#)]
29. Fukano, S.; Arata, T.K.N. Ammonia heat pump package using waste heat as source. In Proceedings of the 4th IIR International Conference on Ammonia Refrigeration Technology, Ohrid, Macedonia, 14–16 April 2011; pp. 2946–2951.
30. Ayub, Z. World’s largest ammonia heat pump (14 MWh) for district heating in Norway—A case study. *Heat Transf. Eng.* **2016**, *37*, 382–386. [[CrossRef](#)]
31. David, A.; Mathiesen, B.V.; Averfalk, H.; Werner, S.; Lund, H. Heat roadmap Europe: Large-scale electric heat pumps in district heating systems. *Energies* **2017**, *10*, 578. [[CrossRef](#)]
32. Taxt Walnum, H.; Sørensen, Å.L.; Ludvigsen, B.; Ivanko, D. Energy consumption for domestic hot water use in Norwegian hotels and nursing homes. *IOP Conf. Ser. Mater. Sci. Eng.* **2019**, *609*, 052020. [[CrossRef](#)]
33. Li, H.; Svendsen, S. Exergy and energy analysis of low temperature district heating network. *Energy* **2012**, *45*, 237–246. [[CrossRef](#)]
34. Larsen, U. (EPTEC Energi AS, Oslo, Norway). Personal communication, 2020.
35. Brekke, S.T. (Therma Industri AS, Oslo, Norway). Personal communication, 2020.

36. Rämä, M.; Sipilä, K. Transition to low temperature distribution in existing systems. *Energy Procedia* **2017**. [[CrossRef](#)]
37. Nord, N.; Løve Nielsen, E.K.; Kauko, H.; Tereshchenko, T. Challenges and potentials for low temperature district heating implementation in Norway. *Energy* **2018**. [[CrossRef](#)]



© 2020 by the authors. Licensee MDPI, Basel, Switzerland. This article is an open access article distributed under the terms and conditions of the Creative Commons Attribution (CC BY) license (<http://creativecommons.org/licenses/by/4.0/>).